

The Dynamics of Particle-Particle Correlations and the Ridge Effect in Proton-Proton Collisions

G. Calé^{1,2}, G. Chachamis^{2,3}, A. Sabio Vera^{4,5}

¹ Departamento de Física, Universidade de Lisboa, Campo Grande 1749-016 Lisboa, Portugal.

² Laboratório de Instrumentação e Física Experimental de Partículas (LIP),
Av. Prof. Gama Pinto, 2, P-1649-003 Lisboa, Portugal.

³ Departamento de Estadística, Informática y Matemáticas,
Universidad Pública de Navarra-UPNA, 31006 Pamplona, Spain.

⁴ Instituto de Física Teórica UAM/CSIC, Nicolás Cabrera 15, E-28049 Madrid, Spain.

⁵ Theoretical Physics Department, Universidad Autónoma de Madrid, E-28049 Madrid, Spain.

May 21, 2024

Abstract

In high-energy particle physics, the study of particle-particle correlations in proton-proton and heavy-ion collisions constitutes a pivotal frontier in the effort to understand the fundamental dynamics of the strong force. To the best of our knowledge, we employ for the first time the BFKL dynamics implemented in a Monte Carlo code in momentum space to compute final state correlations in proton-proton collisions. Our present work aims to investigate whether the particular dynamics of the high-energy limit of QCD can contribute to the long-range rapidity correlations and the enigmatic ridge effect in proton-proton collisions.

1 Introduction

Particle-particle correlations constitute a central aspect of high-energy particle physics, as they enable the exploration of the intricate dynamics of strong force interactions in various collision systems. It is a tool with a long history going back to 1960 when Goldhaber, Goldhaber, Lee and Pais extracted from two-pion correlations the spatial extent of the annihilation fireball in proton-antiproton reactions [1] (for a review, see Ref. [2]).

Particle-particle correlations, in particular correlations in the pseudorapidity-azimuthal angle plane, became anew an extremely important tool for high-energy particle physics in the last 20 years, initially in the analysis of the data from the Relativistic Heavy-Ion Collider (RHIC) at Brookhaven National Laboratory. There, while studying correlations of the final state particles in Au-Au collisions, it was observed the so-called ridge effect, where the produced particles appear as two "ridges" opposite in azimuthal angle ϕ , with approximately flat rapidity distributions [3, 4]. The ridge in ion-ion collisions was seen as a collective phenomenon, namely as a signature of the formation of quark-gluon plasma (QGP) - a hot and dense state of matter [5–7]. The formation of the ridge was explained by the hydrodynamic expansion of the QGP, which creates a pressure gradient that drives the particles to flow along the direction of the collision axis. In other words, the long-range correlations in rapidity for azimuthal angle differences near zero are usually attributed to a collective hydrodynamical flow due to an initial anisotropy in the collision of the two ions

that survives in the distributions of the final-state particles through the collective expansion of the medium [8].

Later, the ridge was also observed at the Large Hadron Collider (LHC) in smaller collision systems, such as proton-proton collisions. The first observation of the ridge effect in proton-proton collisions was reported by the CMS collaboration in 2010, using data from the LHC at a center-of-mass energy of 7 TeV [9]. Long-range correlations have been observed in high-multiplicity proton-proton (pp) [10,11], proton-nucleus (pA) [12–15], and light nucleus-nucleus collisions [16,17]. These findings have raised the question on whether an explanation based on collective phenomena is adequate in hadronic collisions. The formation of a medium and its subsequent evolution, assumed to explain the ridge in heavy-ion collisions, might not apply in small collision systems, since the requirement of thermal equilibrium may not be fulfilled due to the small system size.

Despite the huge theoretical and experimental effort, the ridge effect in proton-proton collisions is still not fully understood [18–20] despite some recent progress [21–23]. At present, most of the possible explanations in the literature involve either the Color Glass Condensate (CGC) framework¹ [25–27] and gluonic flux tubes [28, 29] or hydrodynamic flow [30, 31], while numerous works in the literature offer various descriptions of possible mechanisms responsible for the ridge effect, see for example Refs. [32–38] and references therein.

Recently, a number of experimental studies has given valuable new information but has not resolved the mystery of the ridge effect in small systems. Collective behaviour of final-state hadrons was studied in high-multiplicity events at photoproduction and deep inelastic ep scattering at a centre-of-mass energy of 318 GeV with the ZEUS detector at HERA [39]. In that study, neither the measurements in photoproduction processes nor those in neutral current deep inelastic scattering showed significant collective behaviour similar to what was observed in high-multiplicity hadronic collisions. Furthermore, measurements of two-particle angular correlations of charged particles emitted in hadronic Z decays were presented in Ref. [40]. The analysis was done with archived $e^+ e^-$ annihilation data at a center-of-mass energy of 91 GeV which were collected with the ALEPH detector at LEP. There, no significant enhancement of long-range correlations was observed. A subsequent analysis on data with a center-of-mass energy of up to 209 GeV identified a long-range near-side excess in the correlation function when calculating particle kinematic variables with respect to the thrust axis [41]. Last year, ALICE released a study of the ridge yield measured in a hadronic system of similar multiplicity to the multiplicity of events that come from $e^+ e^-$ annihilation. The ridge yield was substantially larger than what was observed by the ALEPH analysis for center-of-mass energy of 91 GeV. All these are quite indicative that the mechanisms for ridge yield production in very small hadronic systems are not understood and that more theoretical investigation is needed.

With the present work, we want to study whether the QCD dynamics that governs the hardest subprocesses in proton-proton collisions could be responsible for correlations at small azimuthal angles (near side) and large rapidity separations. Typically, in a fixed order calculation, the partonic cross-section is a very low multiplicity event before hadronization, two outgoing partons at leading order (LO), three outgoing partons at next-to-leading order (NLO) and four outgoing partons at next-to-next-to-leading order (NNLO). If the near side correlations were dictated by the hard scattering part, leaving aside the fact that probably one could easily theoretically compute them, we would be able to see them at any multiplicity events which is not the case. On the other hand, going beyond a fixed order calculation for the partonic cross-section, in particular in the high energy limit of QCD (more accurately, the multi-Regge limit), we know that we have the emergence of interesting effects regarding the dominant dynamics, such as the decoupling of the rapidity from the transverse degrees of

¹For a very nice summary, see Ref. [24].

freedom, the reggeization of the t-channel exchanged gluons and rapid increase of the amount of small-x gluons with similar transverse momenta in the colliding protons. Actually, this rapid increase of the number of gluons in the protons eventually leads to unitarity violation at very high energies and the main mechanism to restore the latter is the introduction of parton saturation [42], a key concept within the framework of CGC.

In this paper, we use Monte Carlo simulations to compute the rapidity-azimuthal angle correlations for proton-proton collisions, in particular we use `Pythia8` [43] as a base reference and `BFKLex` which is a Monte Carlo code that generates the hard scattering part of the collision using the the Balitsky-Fadin-Kuraev-Lipatov (BFKL) resummation framework [44–49]. What we aim at with this study is to find out whether any near side correlations arise once we switch from a fixed order + parton shower approach to a BFKL based calculation.

In the next section, we give a short introduction on BFKL and `BFKLex`. In Section 3, we lay the groundwork for our study, we present our results and discuss our findings. In Conclusion, we offer our final remarks and provide insights for future research directions.

2 BFKL and `BFKLex`

An important line of research within particle phenomenology at colliders is to search for effects that are associated with the high energy limit of QCD and to pin down observables that can reveal the effects of the BFKL domain [44–49]. This has proven to be a rather challenging task since the typical phenomenological calculations based on matrix elements computed at fixed order along with the Dokshitzer-Gribov-Lipatov-Altarelli-Parisi (DGLAP) evolution [50–54] to account for the PDFs tend to describe the bulk of the data adequately.

The key idea in this formalism is that, when the center-of-mass energy $\sqrt{s} \rightarrow \infty$, Feynman diagrams that contribute terms of the form $\frac{n}{s} \log^n(s) \sim \frac{n}{s} (y_A - y_B)^n$ give the dominant numerical contributions to the computation of cross-sections. y_A and y_B are the rapidities of some properly chosen tagged particles or jets in the final state, such that their rapidity difference $Y = y_A - y_B$ is the largest among the particles or jets in the final state. The terms $\frac{n}{s} \log^n(s)$ can be of order unity and therefore, these diagrams must be resummed in order to accurately describe experimental observables. In this limit, a decoupling between transverse and longitudinal degrees of freedom takes place which allows to evaluate cross sections in the factorized form:

$$\begin{aligned} LL &= \sum_{n=0}^{\infty} \mathcal{C}_n^{LL} \frac{n}{s} \int_{y_B}^{y_A} dy_1 \int_{y_B}^{y_1} dy_2 \cdots \int_{y_B}^{y_{n-1}} dy_n \\ &= \sum_{n=0}^{\infty} \frac{\mathcal{C}_n^{LL}}{n!} \underbrace{\frac{n}{s} (y_A - y_B)^n}_{LL} \end{aligned}$$

where LL stands for the leading log approximation and y_i correspond to the rapidity of emitted particles. The LL BFKL formalism allows one to calculate the coefficients \mathcal{C}_n^{LL} [44–49]. The next-to-leading log approximation (NLL) [55, 56] is much more complicated since it is sensitive to the running of the strong coupling and to the choice of energy scale in the logarithms. One can parametrize the freedom in the choice of these two scales, respectively, by introducing the constants \mathcal{A} and \mathcal{B} in the previous expression:

$$\begin{aligned} LL+NLL &= \sum_{n=1}^{\infty} \frac{\mathcal{C}_n^{LL}}{n!} \left(\frac{s - \mathcal{A}}{s} \right)^n (y_A - y_B - \mathcal{B})^n \\ &= LL - \sum_{n=1}^{\infty} \frac{(\mathcal{B} \mathcal{C}_n^{LL} + (n-1) \mathcal{A} \mathcal{C}_{n-1}^{LL})}{(n-1)!} \underbrace{\frac{n}{s} (y_A - y_B)^{n-1}}_{NLL} + \dots \end{aligned}$$

We see that at NLL a power in $\log s$ is lost w.r.t. the power of the coupling. Within the formalism, we can then calculate cross sections using the following factorization formula (with $Y \simeq \ln s$)

$$(\mathcal{Q}_1; \mathcal{Q}_2; Y) = \int d^2\mathbf{k}_A d^2\mathbf{k}_B \underbrace{{}_A(\mathcal{Q}_1; \mathbf{k}_A) \quad {}_B(\mathcal{Q}_2; \mathbf{k}_B)}_{\text{PROCESS-DEPENDENT}} \underbrace{f(\mathbf{k}_A; \mathbf{k}_B; Y)}_{\text{UNIVERSAL}};$$

where ${}_A, {}_B$ are process-dependent impact factors which are functions of some external scale, $\mathcal{Q}_{1,2}$, and some internal momentum for reggeized gluons, $\mathbf{k}_{A,B}$. The gluon Green's function f is universal, it depends on $\mathbf{k}_{A,B}$ and on the colliding energy of the process $\sim e^{Y/2}$. It corresponds to the solution of the BFKL equation. In momentum space, the BFKL equation at LL reads

$$\omega f_\omega(\mathbf{k}_A; \mathbf{k}_B) = \omega^2 (\mathbf{k}_A - \mathbf{k}_B) + \int d^2\mathbf{k} \mathcal{K}(\mathbf{k}_A; \mathbf{k}) f_\omega(\mathbf{k}; \mathbf{k}_B); \quad (1)$$

where $\mathcal{K}(\mathbf{k}_a; \mathbf{k})$ is the BFKL kernel

$$\mathcal{K}(\mathbf{k}_a; \mathbf{k}) = \underbrace{2! (-\mathfrak{q}^2)^{-2} (\mathbf{k}_a - \mathbf{k})}_{\mathcal{K}_{\text{virt}}} + \underbrace{\frac{N_c}{2} \frac{s}{(\mathbf{k}_a - \mathbf{k}_b)^2}}_{\mathcal{K}_{\text{real}}}; \quad (2)$$

The solution of the BFKL equation at LL in transverse momentum representation can be written in an iterative form [57] as

$$f = e^{\omega(\vec{k}_A)Y} \left\{ \omega^2 (\mathbf{k}_A - \mathbf{k}_B) + \sum_{n=1}^{\infty} \prod_{i=1}^n \frac{s N_c}{2} \int d^2\mathbf{k}_i \frac{(k_i^2 - \omega^2)}{k_i^2} \int_0^{y_i-1} dy_i e^{(\omega(\vec{k}_A + \sum_{l=1}^i \vec{k}_l) - \omega(\vec{k}_A + \sum_{l=1}^{i-1} \vec{k}_l))y_i} \omega^2 \left(\mathbf{k}_A + \sum_{l=1}^n \mathbf{k}_l - \mathbf{k}_B \right) \right\};$$

where the gluon Regge trajectory reads

$$\omega(\mathfrak{q}) = -\frac{s N_c}{2} \log \frac{\mathfrak{q}^2}{2}$$

and ω is a regulator of infrared divergencies. This solution has been studied at length in a series of papers and it served as the basis in order to construct the Monte Carlo event code **BFKLex** which has had multiple applications in collider phenomenology and more formal studies [58–66]. In this paper, we will run **BFKLex** to LL accuracy.

3 Results and Discussion

Two-particle correlations are analyzed in a two-dimensional azimuthal Δ - Δ phase space, where Δ and Δ denote the difference of the pseudorapidity and the azimuthal angle of the two selected particles, respectively. The two-particle correlation function is defined as

$$C(\Delta; \Delta) = \frac{S(\Delta; \Delta)}{B(\Delta; \Delta)}; \quad (3)$$

where S and B denote particle pair distributions from the same event and from different events respectively, representing the signal and background contributions, see for example

Ref. [67]. As we mentioned in the introduction, one doesn't expect to notice any significant type of near-side correlations just by studying the outgoing partons in a fixed order computation setup. More specifically, since at LO, we have only two outgoing partons flying back to back, we expect these to contribute to the far side ridge since their azimuthal angle difference will be around π . For `Pythia8`, we need to switch on the initial (ISR) and final state radiation (FSR) allowing parton shower. We also switch on multiple partonic interactions (MPI). This will largely increase the number of the quarks and gluons that will eventually hadronise and give the final state hadrons that are typically detected by the LHC experiments. `BFKLex` does not have parton shower implemented. However, we know from the iterative solution described in Section 2 that for medium and large rapidity separations $\Delta = \eta_a - \eta_b$ between the most forward (η_a) and most backward (η_b) partons in BFKL evolution, we have a significant amount of emitted gluons (typically of the order of 15-20) with rapidities $\eta_i: \eta_b < \eta_i < \eta_a$. Furthermore, we will not switch on any MPI scenario when we run `BFKLex`.

In order to be able to qualitatively compare the correlations we compute from `Pythia8` and `BFKLex`, we need to employ the following method: we switch on parton shower in `Pythia8` and we use the anti- k_T clustering algorithm [68] as implemented in `fastjet` [69, 70] to cluster the final state partons (just before hadronization) into minijets. The term minijet was initially used to describe emissions of gluons in the BFKL framework. More precisely, minijets was the term used in the study of dijet production –when the final state is characterized by two jets widely separated in rapidity– to describe any emission activity between the two bounding jets. In particular, we define a minijet as a jet entity with a rapidity value anywhere between the most forward and backward jet rapidities and transverse momentum that can either be large enough e.g. $p_T^{\text{minijet}} > 20$ GeV, to enable experimental detection (thus qualifying as a jet) or much smaller, approaching a few GeV, in which case it appropriately earns its designation as a minijet.

There are two scales we need to set up for the runs. The first one is $\hat{p}_{T,\text{min}}$, which is the lowest allowed p_T for the outgoing partons in the partonic scattering, and the second is $\hat{p}_{T,\text{min}}^{\text{jet}}$, which defines the minimum allowed p_T for a minijet. The former is a parameter passed to the generation of events in `Pythia` whereas the latter is passed to `fastjet` for the clustering. For the hard scattering part of the collision in `BFKLex`, we impose a similar to $\hat{p}_{T,\text{min}}$ low cutoff, which controls the lowest allowed p_T of the most forward and most backward jet or minijet. We decided to use the default PDF set of `Pythia` for all runs in the paper, namely, NNPDF2.3 QCD+QED LO [71]. Despite the fact that is not possible to conduct a realistic experimental analysis on minijets, their study remains of great importance at the theoretical level, offering invaluable insights into fundamental processes.

For the runs with `BFKLex`, we allow the emission of up to 20 gluons in order to compute the gluon Green's function that governs the partonic cross section in the BFKL setup. One could allow for events with an even larger number of final state gluons but such events contribute very little to the total cross section and they do not change the correlation in any visible way. Next, we use again the anti- k_T algorithm to cluster these gluons into minijets. That way, the rapidity-azimuthal angle correlations calculated for minijets above some lower p_T cutoff are infrared safe observables and we can compare the respective distributions from the two Monte Carlo codes.

At this point, it is important to ascertain that the qualitative attributes of the correlation distributions remain intact during the transition from final state minijets to final state partons in our analysis. While it is generally expected that the correlation distributions exhibit similar characteristics when computed for both minijets and final state partons (after parton shower), it is crucial to empirically verify this. To this end, we employ `Pythia8` as a benchmark reference, we calculate the correlations for minijets and for partons and we verify that indeed we observe similar distributions with a noteworthy difference in the region near $\Delta \sim 0$; $\Delta \sim 0$, that can be explained easily due the clustering effects as we

will show in the following. We should also note here that final state partons will undergo hadronization, introducing additional variables to the overall dynamics. Nonetheless, given our current focus on investigating whether the near side ridge originates primarily from dominant QCD dynamics prior to hadronization, concerns regarding hadronization effects are deemed secondary.

In Fig. 1, we present the correlation distribution computed for the final state partons (Left) and the minijets (Right). We observe that there are no long-range correlations in rapidity near $\Delta \sim 0$. This can be seen more clearly in Fig. 2 where we integrate over Δ excluding the range $-2 < \Delta < 2$ to avoid the peak near $\Delta \sim 0$; $\Delta \sim 0$ due to correlations between partons that belong to the same minijet. To be precise, the peak is a characteristic of the parton correlation distribution which turns into a dip once we compute the minijet correlation distribution since there cannot be two minijets closer than $R = 0.5$ in rapidity and azimuthal angle since in that case they would be clustered by **fastjet** into one minijet.

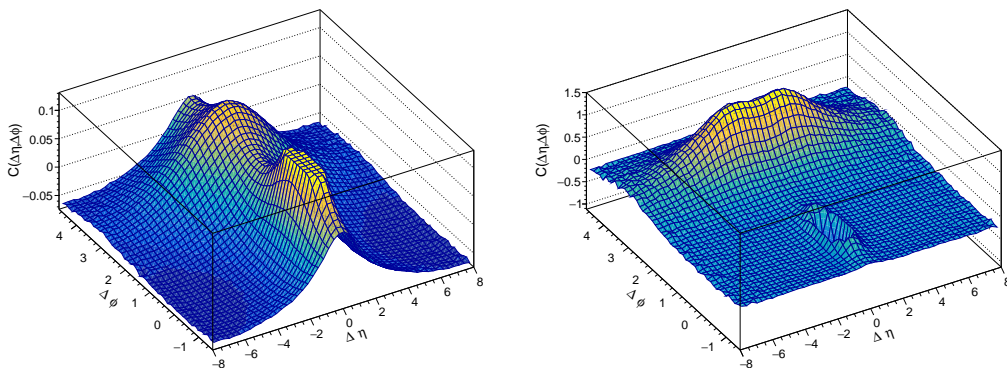


Figure 1: Left: Parton correlation distribution obtained from p-p collisions with **Pythia8**, with a minimum hard process transverse momentum cutoff of $\hat{p}_{T,\min} = 5$ GeV. Right: Minijet correlation distribution obtained from p-p collisions at **Pythia8**, with a minimum hard process transverse momentum cutoff of $\hat{p}_{T,\min} = 5$ GeV. The low p_T cutoff in **fastjet** was set to $p_{T,\min}^{\text{jet}} = 5$ GeV and the jet radius to $R = 0.5$.

In Fig. 3, we present the correlation distribution computed for the minijets with **BFKLex**. We impose a lower p_T cutoff to the most forward and most backward jets, $p_{T,\min} = 5$ GeV. We use two different values for the low p_T cutoff in **fastjet**, $p_{T,\min}^{\text{jet}} = 5$ GeV (Fig. 3, Left) and $p_{T,\min}^{\text{jet}} = 10$ GeV (Fig. 3, Right). As in the case with **Pythia8**, we observe that there are no long-range correlations in rapidity near $\Delta \sim 0$. In Fig. 4, we integrate over Δ excluding the range $-2 < \Delta < 2$ to avoid the dip near $\Delta \sim 0$; $\Delta \sim 0$. We also exclude the intervals $-8 < \Delta < -7$ and $7 < \Delta < 8$ to avoid the statistical fluctuations in Fig. 3 that would only introduce unnecessary noise. We see that the distributions in Fig. 4 are very similar to the ones shown in Fig. 2 (mainly Right).

4 Conclusion

We presented the first BFKL based Monte Carlo study, directly in momentum space, of the rapidity-azimuthal angle correlations between minijets in proton-proton collisions, together with a similar study with **Pythia**, the latter serving as a base reference. We found no

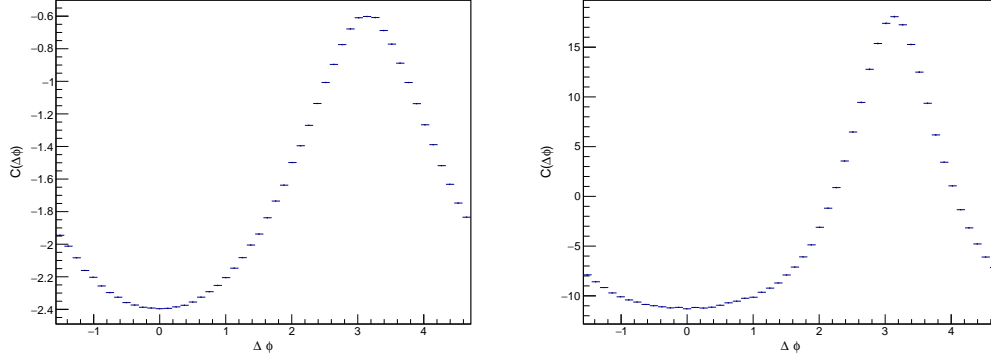


Figure 2: Left: Parton azimuthal correlation distribution obtained after integrating the distribution in Fig. 1 (Left) over $|\Delta| > 2$. Right: Minijet azimuthal correlation distribution obtained after integrating the distribution in Fig. 1 (Right) over $|\Delta| > 2$.

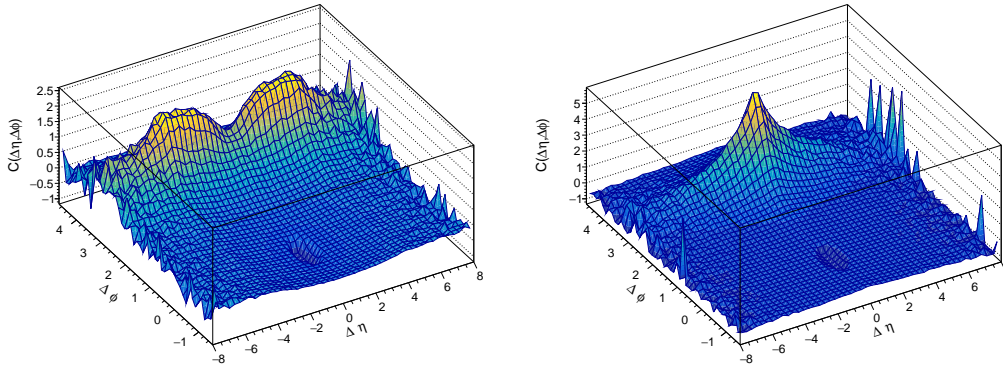


Figure 3: Left: Parton angular correlation distribution obtained from p-p collisions with BFKLex. The minimum transverse momentum cutoff of of the outermost in rapidity jets was set to $p_{T,\min} = 5$ GeV. The low p_T cutoff in `fastjet` was set to $p_{T,\min}^{\text{jet}} = 5$ GeV and the jet radius to $R = 0.5$. Right: The same as to the left with the only difference that the low p_T cutoff in `fastjet` was set to $p_{T,\min}^{\text{jet}} = 10$ GeV

indication that the particular dynamics of the high-energy limit of QCD can be behind the long-range rapidity correlations and the puzzling ridge effect in small systems. It remains to be seen whether this can change with the inclusion of higher order corrections in a full NLL accuracy BFKL analysis.

Acknowledgements

We thank Małgorzata Anna Janik for useful discussions. This work has been supported by the Spanish Research Agency (Agencia Estatal de Investigación) through the grant IFT Centro de Excelencia Severo Ochoa SEV-2016-0597, and by the Spanish Government grant FPA2016-78022-P. It has also received funding from the European Union's Horizon

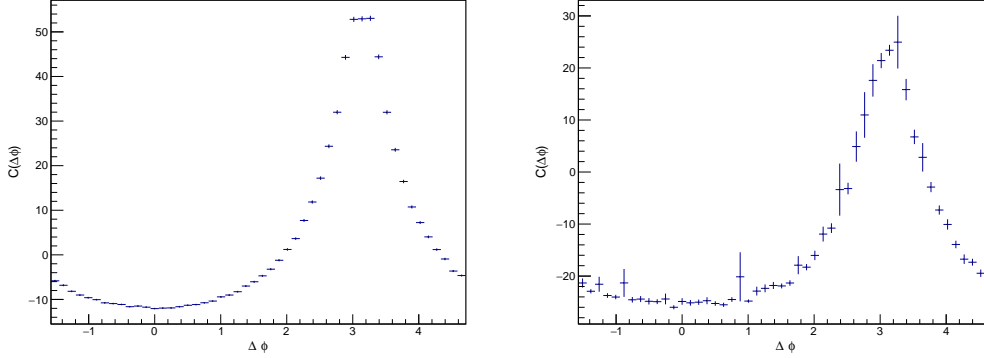


Figure 4: Left: Parton azimuthal correlation distribution obtained after integrating the distribution in Fig. 3 (Left) over $2 < |\Delta| < 7$. Right: Minijet azimuthal correlation distribution obtained after integrating the distribution in Fig. 3 (Right) over $2 < |\Delta| < 7$.

2020 research and innovation programme under grant agreement No. 824093. The work of G.Calé and G.Chachamis was supported by the Fundação para a Ciência e a Tecnologia (Portugal) under project EXPL/FIS-PAR/1195/2021 (<http://doi.org/10.54499/EXPL/FIS-PAR/1195/2021>). G. Chachamis was also supported by the Fundação para a Ciência e a Tecnologia (Portugal) under project CERN/FIS-PAR/0032/2021 (<http://doi.org/10.54499/CERN/FIS-PAR/0032/2021>) and contract ‘Investigador FCT - Individual Call/03216/2017’.

References

- [1] G. Goldhaber, S. Goldhaber, W.-Y. Lee, and A. Pais, “Influence of Bose-Einstein statistics on the anti-proton proton annihilation process,” *Phys. Rev.*, vol. 120, pp. 300–312, 1960.
- [2] U. W. Heinz and B. V. Jacak, “Two particle correlations in relativistic heavy ion collisions,” *Ann. Rev. Nucl. Part. Sci.*, vol. 49, pp. 529–579, 1999.
- [3] J. Adams *et al.*, “Distributions of charged hadrons associated with high transverse momentum particles in pp and Au + Au collisions at $\sqrt{s(NN)} = 200$ -GeV,” *Phys. Rev. Lett.*, vol. 95, p. 152301, 2005.
- [4] J. Putschke, “Intra-jet correlations of high- p_t hadrons from STAR,” *J. Phys. G*, vol. 34, pp. S679–684, 2007.
- [5] L. Van Hove, “THEORETICAL PREDICTION OF A NEW STATE OF MATTER, THE ‘QUARK - GLUON PLASMA’ (ALSO CALLED ‘QUARK MATTER’),” in *17th International Symposium on Multiparticle Dynamics*, pp. 801–818, 1986.
- [6] T. E. O. Ericson, M. R. M. Jacob, H. Satz, and W. J. Willis, “Quark matter formation and heavy ion collisions,” tech. rep., CERN, Geneva, 1982.
- [7] U. W. Heinz and M. Jacob, “Evidence for a new state of matter: An Assessment of the results from the CERN lead beam program,” 1 2000.
- [8] K. Dusling, W. Li, and B. Schenke, “Novel collective phenomena in high-energy proton–proton and proton–nucleus collisions,” *Int. J. Mod. Phys. E*, vol. 25, no. 01, p. 1630002, 2016.

- [9] V. Khachatryan *et al.*, “Observation of Long-Range Near-Side Angular Correlations in Proton-Proton Collisions at the LHC,” *JHEP*, vol. 09, p. 091, 2010.
- [10] G. Aad *et al.*, “Observation of Long-Range Elliptic Azimuthal Anisotropies in $\sqrt{s} = 13$ and 2.76 TeV pp Collisions with the ATLAS Detector,” *Phys. Rev. Lett.*, vol. 116, no. 17, p. 172301, 2016.
- [11] V. Khachatryan *et al.*, “Measurement of long-range near-side two-particle angular correlations in pp collisions at $\sqrt{s} = 13$ TeV,” *Phys. Rev. Lett.*, vol. 116, no. 17, p. 172302, 2016.
- [12] B. Abelev *et al.*, “Long-range angular correlations on the near and away side in p-Pb collisions at $\sqrt{s_{NN}} = 5.02$ TeV,” *Phys. Lett. B*, vol. 719, pp. 29–41, 2013.
- [13] S. Chatrchyan *et al.*, “Observation of Long-Range Near-Side Angular Correlations in Proton-Lead Collisions at the LHC,” *Phys. Lett. B*, vol. 718, pp. 795–814, 2013.
- [14] G. Aad *et al.*, “Measurement of long-range pseudorapidity correlations and azimuthal harmonics in $\sqrt{s_{NN}} = 5.02$ TeV proton-lead collisions with the ATLAS detector,” *Phys. Rev. C*, vol. 90, no. 4, p. 044906, 2014.
- [15] V. Khachatryan *et al.*, “Pseudorapidity dependence of long-range two-particle correlations in pPb collisions at $\sqrt{s_{NN}} = 5.02$ TeV,” *Phys. Rev. C*, vol. 96, no. 1, p. 014915, 2017.
- [16] C. Aidala *et al.*, “Creation of quark–gluon plasma droplets with three distinct geometries,” *Nature Phys.*, vol. 15, no. 3, pp. 214–220, 2019.
- [17] C. Aidala *et al.*, “Measurements of Multiparticle Correlations in d + Au Collisions at 200, 62.4, 39, and 19.6 GeV and p + Au Collisions at 200 GeV and Implications for Collective Behavior,” *Phys. Rev. Lett.*, vol. 120, no. 6, p. 062302, 2018.
- [18] M. Strickland, “Small system studies: A theory overview,” *Nucl. Phys. A*, vol. 982, pp. 92–98, 2019.
- [19] C. Loizides, “Experimental overview on small collision systems at the LHC,” *Nucl. Phys. A*, vol. 956, pp. 200–207, 2016.
- [20] J. L. Nagle and W. A. Zajc, “Small System Collectivity in Relativistic Hadronic and Nuclear Collisions,” *Ann. Rev. Nucl. Part. Sci.*, vol. 68, pp. 211–235, 2018.
- [21] B. Schenke, C. Shen, and P. Tribedy, “Running the gamut of high energy nuclear collisions,” *Phys. Rev. C*, vol. 102, no. 4, p. 044905, 2020.
- [22] W. Zhao, S. Ryu, C. Shen, and B. Schenke, “3D structure of anisotropic flow in small collision systems at energies available at the BNL Relativistic Heavy Ion Collider,” *Phys. Rev. C*, vol. 107, no. 1, p. 014904, 2023.
- [23] M. I. Abdulhamid *et al.*, “Measurements of the Elliptic and Triangular Azimuthal Anisotropies in Central He3+Au, d+Au and p+Au Collisions at sNN=200 GeV,” *Phys. Rev. Lett.*, vol. 130, no. 24, p. 242301, 2023.
- [24] T. Altinoluk and N. Armesto, “Particle correlations from the initial state,” *Eur. Phys. J. A*, vol. 56, no. 8, p. 215, 2020.
- [25] J. Jalilian-Marian, A. Kovner, A. Leonidov, and H. Weigert, “The Wilson renormalization group for low x physics: Towards the high density regime,” *Phys. Rev. D*, vol. 59, p. 014014, 1998.

- [26] E. Iancu, A. Leonidov, and L. McLerran, “The Color glass condensate: An Introduction,” in *Cargese Summer School on QCD Perspectives on Hot and Dense Matter*, pp. 73–145, 2 2002.
- [27] F. Gelis, E. Iancu, J. Jalilian-Marian, and R. Venugopalan, “The Color Glass Condensate,” *Ann. Rev. Nucl. Part. Sci.*, vol. 60, pp. 463–489, 2010.
- [28] A. Dumitriu, F. Gelis, L. McLerran, and R. Venugopalan, “Glasma flux tubes and the near side ridge phenomenon at RHIC,” *Nucl. Phys. A*, vol. 810, pp. 91–108, 2008.
- [29] S. D. Glazek, S. J. Brodsky, A. S. Goldhaber, and R. W. Brown, “Ridge effect, azimuthal correlations, and other novel features of gluonic string collisions in high energy photon-mediated reactions,” *Phys. Rev. D*, vol. 97, no. 11, p. 114021, 2018.
- [30] A. Bzdak, B. Schenke, P. Tribedy, and R. Venugopalan, “Initial state geometry and the role of hydrodynamics in proton-proton, proton-nucleus and deuteron-nucleus collisions,” *Phys. Rev. C*, vol. 87, no. 6, p. 064906, 2013.
- [31] K. Werner, I. Karpenko, and T. Pierog, “The ‘Ridge’ in Proton-Proton Scattering at 7 TeV,” *Phys. Rev. Lett.*, vol. 106, p. 122004, 2011.
- [32] J. D. Bjorken, S. J. Brodsky, and A. Scharff Goldhaber, “Possible multiparticle ridge-like correlations in very high multiplicity proton-proton collisions,” *Phys. Lett. B*, vol. 726, pp. 344–346, 2013.
- [33] W. Li, “Observation of a ‘Ridge’ correlation structure in high multiplicity proton-proton collisions: A brief review,” *Mod. Phys. Lett. A*, vol. 27, p. 1230018, 2012.
- [34] N. Armesto, C. A. Salgado, and U. A. Wiedemann, “Measuring the collective flow with jets,” *Phys. Rev. Lett.*, vol. 93, p. 242301, 2004.
- [35] A. Majumder, B. Muller, and S. A. Bass, “Longitudinal Broadening of Quenched Jets in Turbulent Color Fields,” *Phys. Rev. Lett.*, vol. 99, p. 042301, 2007.
- [36] P. Romatschke, “Momentum broadening in an anisotropic plasma,” *Phys. Rev. C*, vol. 75, p. 014901, 2007.
- [37] E. V. Shuryak, “On the origin of the ‘Ridge’ phenomenon induced by jets in heavy ion collisions,” *Phys. Rev. C*, vol. 76, p. 047901, 2007.
- [38] E. Musumeci, A. Irls, R. Perez-Ramos, I. Corredoira, E. Sarkisyan-Grinbaum, V. A. Mitsou, and M. A. Sanchis-Lozano, “Exploring hidden sectors with two-particle angular correlations at future e^+e^- colliders,” 12 2023.
- [39] I. Abt *et al.*, “Azimuthal correlations in photoproduction and deep inelastic ep scattering at HERA,” *JHEP*, vol. 12, p. 102, 2021.
- [40] A. Badea, A. Baty, P. Chang, G. M. Innocenti, M. Maggi, C. McGinn, M. Peters, T.-A. Sheng, J. Thaler, and Y.-J. Lee, “Measurements of two-particle correlations in e^+e^- collisions at 91 GeV with ALEPH archived data,” *Phys. Rev. Lett.*, vol. 123, no. 21, p. 212002, 2019.
- [41] Y.-C. Chen *et al.*, “Long-range near-side correlation in e^+e^- Collisions at 183-209 GeV with ALEPH Archived Data,” 12 2023.
- [42] L. V. Gribov, E. M. Levin, and M. G. Ryskin, “Semihard Processes in QCD,” *Phys. Rept.*, vol. 100, pp. 1–150, 1983.

- [43] C. Bierlich *et al.*, “A comprehensive guide to the physics and usage of PYTHIA 8.3,” *SciPost Phys. Codeb.*, vol. 2022, p. 8, 2022.
- [44] L. N. Lipatov, “The Bare Pomeron in Quantum Chromodynamics,” *Sov. Phys. JETP*, vol. 63, pp. 904–912, 1986.
- [45] I. I. Balitsky and L. N. Lipatov, “The Pomernanchuk Singularity in Quantum Chromodynamics,” *Sov. J. Nucl. Phys.*, vol. 28, pp. 822–829, 1978.
- [46] E. A. Kuraev, L. N. Lipatov, and V. S. Fadin, “The Pomernanchuk Singularity in Non-abelian Gauge Theories,” *Sov. Phys. JETP*, vol. 45, pp. 199–204, 1977.
- [47] E. A. Kuraev, L. N. Lipatov, and V. S. Fadin, “Multi - Reggeon Processes in the Yang-Mills Theory,” *Sov. Phys. JETP*, vol. 44, pp. 443–450, 1976.
- [48] L. N. Lipatov, “Reggeization of the Vector Meson and the Vacuum Singularity in Non-abelian Gauge Theories,” *Sov. J. Nucl. Phys.*, vol. 23, pp. 338–345, 1976.
- [49] V. S. Fadin, E. A. Kuraev, and L. N. Lipatov, “On the Pomernanchuk Singularity in Asymptotically Free Theories,” *Phys. Lett. B*, vol. 60, pp. 50–52, 1975.
- [50] V. N. Gribov and L. N. Lipatov, “Deep inelastic e p scattering in perturbation theory,” *Sov. J. Nucl. Phys.*, vol. 15, pp. 438–450, 1972.
- [51] V. N. Gribov and L. N. Lipatov, “e+ e- pair annihilation and deep inelastic e p scattering in perturbation theory,” *Sov. J. Nucl. Phys.*, vol. 15, pp. 675–684, 1972.
- [52] L. N. Lipatov, “The parton model and perturbation theory,” *Yad. Fiz.*, vol. 20, pp. 181–198, 1974.
- [53] G. Altarelli and G. Parisi, “Asymptotic Freedom in Parton Language,” *Nucl. Phys. B*, vol. 126, pp. 298–318, 1977.
- [54] Y. L. Dokshitzer, “Calculation of the Structure Functions for Deep Inelastic Scattering and e+ e- Annihilation by Perturbation Theory in Quantum Chromodynamics,” *Sov. Phys. JETP*, vol. 46, pp. 641–653, 1977.
- [55] V. S. Fadin and L. N. Lipatov, “BFKL pomeron in the next-to-leading approximation,” *Phys. Lett. B*, vol. 429, pp. 127–134, 1998.
- [56] M. Ciafaloni and G. Camici, “Energy scale(s) and next-to-leading BFKL equation,” *Phys. Lett. B*, vol. 430, pp. 349–354, 1998.
- [57] C. R. Schmidt, “A Monte Carlo solution to the BFKL equation,” *Phys. Rev. Lett.*, vol. 78, pp. 4531–4535, 1997.
- [58] G. Chachamis and A. Sabio Vera, “On the conformal spin dependence of the perturbative QCD vacuum singularity,” *JHEP*, vol. 07, p. 109, 2022.
- [59] N. B. de León, G. Chachamis, and A. Sabio Vera, “Multiperipheral final states in crowded twin-jet events at the LHC,” *Nucl. Phys. B*, vol. 971, p. 115518, 2021.
- [60] G. Chachamis and A. Sabio Vera, “The high-energy radiation pattern from BFKLex with double-log collinear contributions,” *JHEP*, vol. 02, p. 064, 2016.
- [61] G. Chachamis and A. Sabio Vera, “Monte Carlo study of double logarithms in the small x region,” *Phys. Rev. D*, vol. 93, no. 7, p. 074004, 2016.

- [62] F. Caporale, G. Chachamis, J. D. Madrigal, B. Murdaca, and A. Sabio Vera, “A study of the diffusion pattern in $N = 4$ SYM at high energies,” *Phys. Lett. B*, vol. 724, pp. 127–132, 2013.
- [63] G. Chachamis, A. Sabio Vera, and C. Salas, “Bootstrap and momentum transfer dependence in small x evolution equations,” *Phys. Rev. D*, vol. 87, no. 1, p. 016007, 2013.
- [64] G. Chachamis and A. Sabio Vera, “The NLO $N = 4$ SUSY BFKL Green function in the adjoint representation,” *Phys. Lett. B*, vol. 717, pp. 458–461, 2012.
- [65] G. Chachamis and A. Sabio Vera, “The Colour Octet Representation of the Non-Forward BFKL Green Function,” *Phys. Lett. B*, vol. 709, pp. 301–308, 2012.
- [66] G. Chachamis, M. Deak, A. Sabio Vera, and P. Stephens, “A Comparative study of small x Monte Carlos with and without QCD coherence effects,” *Nucl. Phys. B*, vol. 849, pp. 28–44, 2011.
- [67] A. Adare *et al.*, “Dihadron azimuthal correlations in Au+Au collisions at $\sqrt{s_{NN}} = 200$ GeV,” *Phys. Rev. C*, vol. 78, p. 014901, 2008.
- [68] M. Cacciari, G. P. Salam, and G. Soyez, “The anti- k_t jet clustering algorithm,” *JHEP*, vol. 04, p. 063, 2008.
- [69] M. Cacciari, G. P. Salam, and G. Soyez, “FastJet User Manual,” *Eur. Phys. J. C*, vol. 72, p. 1896, 2012.
- [70] M. Cacciari and G. P. Salam, “Dispelling the N^3 myth for the k_t jet-finder,” *Phys. Lett. B*, vol. 641, pp. 57–61, 2006.
- [71] R. D. Ball, V. Bertone, S. Carrazza, L. Del Debbio, S. Forte, A. Guffanti, N. P. Hartland, and J. Rojo, “Parton distributions with QED corrections,” *Nucl. Phys. B*, vol. 877, pp. 290–320, 2013.